

The curious case of HD41248. A pair of static signals buried behind red-noise¹

J.S. Jenkins¹ and M. Tuomi^{1,2,3}

¹*Departamento de Astronomía, Universidad de Chile, Camino el Observatorio 1515, Las Condes, Santiago, Chile, Casilla 36-D*

²*Center for Astrophysics, University of Hertfordshire, College Lane Campus, Hatfield, Hertfordshire, UK, AL10 9AB*

³*University of Turku, Tuorla Observatory, Department of Physics and Astronomy, Väisäläntie 20, FI-21500, Piikkiö, Finland*

ABSTRACT

Gaining a better understanding of the effects of stellar induced radial velocity noise is critical for the future of exoplanet studies, since the discovery of the lowest-mass planets using this method will require us to go below the intrinsic stellar noise limit. An interesting test case in this respect is that of the southern solar analogue HD41248. The radial velocity time series of this star has been proposed to contain either a pair of signals with periods of around 18 and 25 days, that could be due to a pair of resonant super-Earths, or a single and varying 25 day signal that could arise due to a complex interplay between differential rotation and modulated activity. In this letter we build-up more evidence for the former scenario, showing that the signals are still clearly significant even after more than 10 years of observations and they likely do not change in period, amplitude, or phase as a function of time, the hallmarks of static Doppler signals. We show that over the last two observing seasons this star was more intrinsically active and the noise reddened, highlighting why better noise models are needed to find the lowest amplitude signals, in particular models that consider noise correlations. This analysis shows that there is still sufficient evidence for the existence of two super-Earths on the edge of, or locked into, a 7:5 mean motion resonance orbiting HD41248.

Subject headings: stars: fundamental parameters — stars: (HD41248) — stars: rotation — (stars:) planetary systems

1. Introduction

The discovery of low-mass planets in the super-Earth regime using the radial velocity method is at the forefront of modern exoplanet science as it pushes the boundaries of what is possible using current technology (Pepe et al. 2011; Tuomi et al. 2014b; Anglada-Escudé et al. 2013). However, the Doppler signals imposed on the host stars of such orbiting bodies can also be fighting for dominance with signals induced in the data by rotationally modulated activity features like star spots (see Boisse et al. 2011).

A radial velocity analysis of the star HD166435 by Queloz et al. (2001) found a repeating short period signal of less than 4 days, suggesting the presence of a planetary companion to the star. After photometric follow-up they found a period matching the period of the radial velocity signal, indicating the star was actually active and the signal they had detected was due to rotationally modulated star spots. This was confirmed when they found that the coherence time of the radial velocity signal was only ~ 30 days and correlations were found with the bisector inverse slope (BIS), meaning it was not a static signal as expected of a genuine Doppler velocity profile.

¹Email: jjenkins@das.uchile.cl

GJ581 provides another example of false-positive radial velocity signals where a possible candidate planet (GJ581 d) was reported in Udry et al. (2007) with a period of 82 days, later shown to be the 1-year alias of another planet candidate period of 67 days (Mayor et al. 2009). The existence of the habitable zone super-Earth GJ581 g (Vogt et al. 2010) has also been disputed (Tuomi 2012; Baluev 2013; Hatzes 2013a), later countered by Vogt et al. (2012), as has the existence of the Earth-mass planet reported to be orbiting Alpha Cen B (Dumusque et al. 2012; Hatzes 2013b). Clearly the detection of low-mass planets approaching the intrinsic noise level of the star and instrument combination is fraught with difficulty.

Jenkins et al. (2013b) announced the discovery of a pair of planetary candidates orbiting the star HD41248 in, or close to a 7:5 mean motion resonance (MMR) configuration. Both signals reported in their work were statistically significant, even when considering correlations between the activity indicators and the radial velocities. However, although the time baseline was long, around 7.5 years, they only had a total of 62 Doppler velocities, yet the MMR configuration (period ratio of 1.400 ± 0.002) seemed to favour a planetary hypothesis as such a pair of periods so close to a 7:5 integer ratio seems difficult to attribute to the star. The metal-poor nature of HD41248 ($[\text{Fe}/\text{H}] = -0.43$ dex) also agrees with the emerging notion that metal-poor stars have a higher fraction of the lowest-mass planets (Jenkins et al. 2013a).

Recently, Santos et al. (2014) have claimed that the longer period signal in the HD41248 radial velocity data is likely due to rotationally modulated magnetic activity, after adding more than 160 new velocities, and when subtracting off that signal, there is no remaining evidence for the 18 day signal. With this in mind we decided to re-analyze all data for HD41248 and test whether the pair of signals still remain in the new data from Santos et al. Moreover, we discuss whether these signals could still be interpreted as being due to a pair of planets.

2. HD41248 Statistical Model

We modelled the HARPS radial velocities of HD42148 by adopting the analysis techniques

and the statistical model applied in Tuomi et al. (2014a). This model contains Keplerian signals, a linear trend, moving average component with exponential smoothing, and linear correlations with activity indices, namely, BIS, full width at half maximum (FWHM), and chromospheric activity S -index. According to Tuomi et al. such a model can filter out activity-related variations in radial velocities and even suppress the velocity variations caused by the co-rotation of star spots on the stellar surface below the detection threshold, enabling the detection of low-amplitude variations of planetary origin, as witnessed on CoRoT-7 (Tuomi et al.). We write the statistical model as

$$m_{i,l} = \gamma_l + \dot{\gamma}t_i + f_k(t_i) + \epsilon_{i,l} + \sum_{j=1}^q c_{j,l} \xi_{j,i,l} + \sum_{j=1}^p \phi_{j,l} \exp\left\{\frac{t_{i-j} - t_i}{\tau_l}\right\} \epsilon_{i,l}, \quad (1)$$

where $m_{i,l}$ is the measurement made at time t_i and the index l denotes that it corresponds to an independent l th data set, parameter γ_l is the reference velocity, function f_k denotes the superposition of k Keplerian signals, $\epsilon_{i,l}$ is a Gaussian white noise with zero mean and a variance of $\sigma_i^2 + \sigma_l^2$, where σ_i is the estimated instrument uncertainty corresponding to the radial velocity measurement $m_{i,l}$ and σ_l quantifies the excess white noise in the l th data set, parameters $c_{j,l}$ describe the linear correlations with the activity indices $\xi_{j,i,l}$, for $j = 1, \dots, q$, and parameters $\phi_{j,l}$ quantify the moving average components, $j = 1, \dots, p$, with exponential smoothing in a time-scale of τ_l . In practice we apply a first-order moving average model (MA(1)) as we believe it is a sufficiently accurate description of this data, parameterised by setting the moving average components (p) in Eqⁿ 1 equal to unity.

The prior probability densities have to be defined in order to use the techniques of Tuomi et al. (2014a) relying on the Bayes' rule of conditional probabilities. We define these densities according to Tuomi & Anglada-Escudé (2013) by choosing uninformative and uniform densities for all but two model parameters, namely the eccentricities (e) and excess jitter (σ_j). These are set such that low eccentricities and low jitters are preferred

but that higher values are not ruled out *a priori* (Tuomi et al. 2014a).

As the noise caused by inhomogeneities of the stellar surface and activity cannot be expected to be time-invariant over the baseline of the observations of over ten years, we model the velocities already analysed in (Jenkins et al. 2013b) and the new ones obtained during the last two years as independent data sets. In this way, we can account for the possibility that the noise properties have changed over the data baseline and the potential effects that the data sampling, which is more dense during the last two years, has on the parameters of the noise model. Finally, we also split the last two observing seasons up into two subsets of data, and although this is detrimental to the information content, this was done to directly compare our results with those recently published in Santos et al. (2014).

3. HD41248 Reanalysis

We applied our statistical model outlined above to the full dataset of radial velocities for HD41248, combining the previously published data in Jenkins et al. (2013b) with the newly published data in Santos et al. (2014), giving rise to a total timeseries of 223 HARPS (Mayor et al. 2003) velocities². We applied both tests with and without including the linear activity correlation terms and also compared to the white noise model applied in Santos et al. Table 1 contains the measured radial velocities, BIS and FWHM values from the HARPS CCFs, and the chromospheric *S*-indices that were measured following the procedures in Jenkins et al. (2006, 2008, 2011).

²The data were obtained from the European Southern Observatory archive under the request number JJENKINS-110394.

TABLE 1
HARPS TIMESERIES DATA FOR HD41248.

BJD	RV [ms ⁻¹]	S-index [dex]	BIS [ms ⁻¹]	FWHM [ms ⁻¹]
2452943.8528426	3526.59±2.59	0.169	35.93	6721.78
2452989.7102293	3519.14±4.06	0.170	27.40	6719.01
2452998.6898180	3526.43±5.43	0.179	33.53	6701.21
2453007.6786518	3526.63±2.53	0.162	28.61	6718.20
2453787.6079555	3522.44±2.76	0.162	31.31	6718.54
2454055.8375443	3523.18±2.06	0.168	23.95	6714.52
2454789.7207967	3522.99±0.82	0.171	27.43	6722.19
2454790.6943362	3519.49±0.90	0.170	30.83	6724.20
2454791.7055725	3522.47±0.83	0.171	29.54	6720.60
2454792.7042506	3522.29±0.80	0.172	28.09	6728.65
2454793.7211230	3524.99±0.89	0.173	25.28	6727.73
2454794.6946036	3527.04±0.89	0.172	29.59	6732.04
2454795.7156306	3528.45±0.91	0.174	29.54	6725.92
2454796.7195391	3528.21±0.96	0.174	30.33	6727.87
2454797.7051254	3528.99±0.91	0.175	27.77	6733.22
2454798.6972277	3531.20±0.92	0.173	25.14	6731.22
2454902.5907553	3525.08±2.02	0.180	21.34	6729.23
2454903.5172666	3527.59±0.78	0.172	27.69	6726.66
2454904.5185682	3525.76±0.90	0.174	27.19	6722.67
2454905.5355291	3527.55±0.90	0.171	27.98	6722.94
2454906.5179999	3527.95±1.04	0.171	31.02	6723.86
2454907.5647983	3527.52±0.91	0.173	28.88	6727.05
2454908.5603822	3526.23±0.80	0.172	27.95	6720.84
2454909.5380036	3527.11±0.85	0.170	25.45	6721.36
2454910.5385064	3528.24±1.12	0.173	27.51	6726.82
2454911.5427244	3524.98±0.75	0.172	28.13	6721.05
2454912.5392921	3525.22±0.74	0.172	25.78	6718.78
2455284.5272133	3528.23±0.73	0.175	28.43	6724.46
2455287.5109103	3524.60±0.88	0.174	25.19	6733.01
2455288.5285775	3523.32±0.75	0.173	25.44	6730.41
2455289.5460248	3526.70±0.79	0.174	26.29	6723.60
2455290.5095380	3525.90±0.89	0.174	21.96	6727.32
2455291.5216615	3526.08±1.01	0.171	26.86	6734.67
2455293.5043818	3527.36±0.97	0.172	27.39	6727.22
2455304.5180173	3522.41±1.69	0.144	31.21	6801.23
2455328.4550220	3529.11±0.79	0.175	20.74	6735.39
2455334.4564390	3532.00±1.37	0.169	25.33	6737.32
2455387.9305071	3530.98±1.04	0.171	27.29	6737.65
2455390.9312188	3531.33±1.58	0.164	30.24	6734.98
2455434.8790630	3516.75±3.33	0.157	31.59	6740.53
2455439.8843407	3527.76±3.26	0.159	32.81	6723.48

TABLE 1—*Continued*

BJD	RV [ms ⁻¹]	S-index [dex]	BIS [ms ⁻¹]	FWHM [ms ⁻¹]
2455445.9241644	3522.93±3.11	0.162	28.31	6727.79
2455465.8566225	3526.62±1.41	0.171	23.18	6731.85
2455480.8795598	3527.59±1.13	0.171	27.10	6728.47
2455483.8136024	3525.01±1.74	0.170	27.97	6734.02
2455488.8262312	3525.84±0.75	0.171	31.08	6725.48
2455494.8532009	3529.81±0.95	0.169	26.88	6730.95
2455513.7823100	3528.86±1.29	0.172	35.60	6740.83
2455516.7515789	3530.74±0.94	0.175	22.72	6736.79
2455519.7046533	3528.85±1.20	0.168	21.96	6735.81
2455537.7997291	3527.71±0.72	0.176	27.01	6730.30
2455545.7213656	3529.20±0.85	0.175	26.69	6737.60
2455549.7548559	3527.95±0.83	0.171	31.98	6734.55
2455576.7923481	3525.35±1.01	0.165	29.18	6733.68
2455580.7312518	3519.41±0.90	0.169	32.95	6729.42
2455589.7734088	3528.42±1.42	0.169	24.59	6733.73
2455612.6068850	3527.66±0.82	0.171	25.59	6731.09
2455623.6361828	3528.30±1.18	0.169	28.96	6726.23
2455629.5528393	3528.65±0.94	0.168	25.71	6732.35
2455641.5542106	3528.98±1.01	0.170	28.91	6727.21
2455644.5845033	3529.35±1.26	0.174	19.09	6740.11
2455647.5796694	3529.95±1.37	0.167	29.11	6737.56
2455904.8445150	3523.18±2.58	0.158	40.69	6747.45
2456215.8328718	3526.25±1.39	0.168	30.20	6743.55
2456218.7962306	3524.50±1.84	0.164	28.94	6740.25
2456218.8693916	3523.75±1.62	0.165	35.11	6739.30
2456220.8683473	3524.85±1.09	0.163	25.77	6731.64
2456229.7183898	3532.26±1.69	0.166	31.33	6740.83
2456229.8714013	3527.06±1.40	0.166	29.16	6736.86
2456230.6857996	3530.13±1.47	0.167	27.20	6743.88
2456230.8458134	3531.97±1.34	0.167	28.59	6736.59
2456231.7334650	3531.02±1.55	0.171	29.46	6749.04
2456231.8607353	3529.80±1.20	0.168	28.35	6741.43
2456236.6604420	3524.84±1.51	0.173	29.56	6745.23
2456236.8633497	3524.75±1.19	0.174	33.24	6733.75
2456237.6662421	3525.98±1.33	0.177	28.27	6738.88
2456237.8808398	3525.49±0.90	0.176	26.42	6741.69
2456238.6619956	3532.88±1.31	0.175	29.30	6746.51
2456238.6977368	3527.82±1.33	0.173	28.61	6742.04
2456239.6522975	3532.63±1.42	0.175	24.85	6747.45
2456245.7084222	3525.35±1.09	0.173	24.69	6743.09
2456247.6418575	3528.74±1.02	0.168	28.32	6741.03

TABLE 1—*Continued*

BJD	RV [ms ⁻¹]	S-index [dex]	BIS [ms ⁻¹]	FWHM [ms ⁻¹]
2456256.6533194	3532.39±2.19	0.167	24.63	6747.43
2456256.7645704	3525.52±1.24	0.175	25.11	6732.43
2456257.6680498	3533.01±1.16	0.173	23.79	6744.10
2456257.8001458	3530.94±1.23	0.178	32.49	6743.71
2456258.7216343	3527.87±1.51	0.171	19.43	6747.10
2456258.7556855	3529.95±1.47	0.173	29.98	6746.68
2456259.7335053	3524.76±1.30	0.175	23.97	6746.34
2456259.7520008	3525.54±1.26	0.175	23.55	6745.35
2456262.6948682	3529.96±1.62	0.176	25.69	6742.39
2456262.7981443	3523.17±1.32	0.178	27.46	6732.01
2456263.6232652	3532.22±1.51	0.174	26.24	6741.81
2456263.8103729	3529.64±1.14	0.174	24.40	6748.01
2456307.5801789	3532.77±1.00	0.171	27.54	6743.34
2456307.7092172	3533.96±1.33	0.180	24.02	6749.01
2456308.5535163	3530.95±1.08	0.176	28.15	6736.73
2456308.8012459	3533.41±1.41	0.170	24.73	6739.00
2456309.5762513	3533.01±1.10	0.178	28.63	6744.66
2456309.7930203	3531.16±1.28	0.172	31.86	6747.49
2456310.5910230	3532.02±1.19	0.177	18.72	6741.44
2456310.7069248	3536.34±1.26	0.177	19.30	6738.18
2456311.5625541	3532.26±1.34	0.171	28.39	6747.14
2456311.6578889	3530.72±1.20	0.176	28.15	6742.01
2456312.5914918	3529.65±1.26	0.174	26.59	6741.52
2456312.7438284	3534.54±2.32	0.169	17.33	6759.18
2456314.5898762	3531.61±1.61	0.176	24.95	6757.65
2456314.7537057	3530.93±1.62	0.173	28.79	6755.44
2456315.6175515	3528.47±2.03	0.191	31.34	6756.00
2456315.7297379	3528.90±1.58	0.184	23.65	6749.19
2456316.6766846	3532.46±1.57	0.182	19.56	6745.99
2456317.5901359	3526.93±1.14	0.173	23.48	6745.87
2456317.6744291	3530.39±1.27	0.171	21.48	6743.95
2456318.5677531	3529.95±1.37	0.173	28.49	6741.46
2456318.6886662	3535.64±2.18	0.185	26.26	6752.97
2456319.5818048	3526.20±1.52	0.178	26.31	6736.50
2456319.7199515	3517.28±2.59	0.178	36.77	6759.41
2456320.6218166	3526.41±1.13	0.174	32.82	6739.65
2456320.7117346	3526.74±1.60	0.172	23.78	6736.66
2456321.6454163	3527.10±1.74	0.174	26.13	6744.54
2456321.7454383	3526.19±1.56	0.174	27.20	6744.40
2456326.5925681	3526.19±1.65	0.172	32.18	6744.18
2456326.6716412	3524.07±1.65	0.178	25.37	6736.35

TABLE 1—*Continued*

BJD	RV [ms ⁻¹]	S-index [dex]	BIS [ms ⁻¹]	FWHM [ms ⁻¹]
2456354.5410577	3527.23±1.13	0.165	32.33	6731.94
2456354.6178620	3522.61±1.82	0.169	26.08	6735.38
2456357.5276034	3529.82±1.59	0.166	29.62	6745.95
2456357.6455296	3530.10±1.42	0.163	23.82	6742.41
2456362.5180018	3528.99±1.14	0.175	27.93	6737.80
2456362.6121205	3528.42±1.28	0.177	25.45	6744.41
2456366.5017386	3526.21±0.98	0.175	24.63	6731.86
2456366.6539234	3527.18±2.20	0.174	25.56	6758.16
2456383.5228456	3527.32±1.81	0.173	27.84	6743.47
2456384.5783826	3531.49±1.66	0.163	17.53	6734.83
2456385.4956349	3526.67±1.34	0.165	25.32	6732.94
2456385.5663744	3529.43±1.84	0.168	30.42	6741.01
2456386.4894948	3529.38±1.39	0.168	24.65	6741.94
2456386.5607204	3527.55±1.25	0.164	22.69	6737.07
2456387.5267452	3527.35±1.27	0.180	26.54	6738.97
2456387.5630872	3526.19±1.49	0.170	28.71	6742.92
2456389.4913755	3530.50±1.22	0.170	28.87	6737.10
2456389.5578790	3529.82±1.34	0.168	30.95	6741.93
2456390.4892403	3528.62±1.35	0.170	27.67	6740.02
2456390.5645400	3527.94±1.32	0.170	25.35	6743.67
2456394.5131767	3520.93±1.34	0.166	29.75	6742.50
2456397.5056966	3522.49±1.36	0.165	28.01	6737.56
2456399.5231059	3524.07±1.05	0.172	30.15	6735.54
2456402.5030123	3528.33±1.06	0.168	30.25	6739.08
2456409.4955108	3530.07±7.47	0.205	39.30	6717.70
2456414.4684733	3532.52±1.19	0.170	23.77	6743.40
2456521.9016581	3525.91±1.32	0.168	26.89	6749.61
2456524.9204178	3527.03±0.92	0.174	31.13	6744.43
2456525.9077938	3533.12±2.05	0.165	22.16	6744.49
2456526.9330524	3525.49±1.04	0.170	30.36	6745.33
2456534.9211421	3525.52±0.85	0.169	26.82	6736.37
2456538.8521797	3536.99±1.65	0.167	29.80	6750.23
2456538.9215906	3530.71±1.35	0.171	25.16	6741.72
2456539.9012946	3532.42±1.59	0.174	28.36	6747.01
2456542.9158485	3529.81±1.42	0.170	33.66	6748.92
2456543.9208079	3531.25±1.08	0.174	24.88	6748.21
2456564.7508993	3531.65±1.78	0.166	26.35	6745.64
2456564.9043048	3534.39±1.82	0.166	25.79	6751.38
2456565.7808829	3532.73±0.93	0.171	30.83	6747.99
2456565.8439396	3531.39±1.82	0.168	27.50	6746.86
2456585.7655987	3524.51±1.20	0.171	27.67	6746.72

TABLE 1—*Continued*

BJD	RV [ms ⁻¹]	S-index [dex]	BIS [ms ⁻¹]	FWHM [ms ⁻¹]
2456585.8490838	3523.68±1.04	0.171	33.58	6746.03
2456586.7691910	3530.26±1.61	0.169	25.38	6746.28
2456586.8643661	3528.84±1.11	0.173	29.25	6738.47
2456589.8651653	3531.07±0.92	0.175	33.10	6740.17
2456590.7783506	3529.10±1.47	0.170	31.50	6751.98
2456590.8722988	3533.43±1.38	0.168	25.97	6756.39
2456591.7566178	3532.10±1.58	0.175	23.82	6751.30
2456591.8177645	3531.08±1.27	0.174	26.57	6754.02
2456592.7146993	3534.20±1.23	0.174	26.47	6751.38
2456592.8521782	3533.31±1.03	0.178	24.86	6743.74
2456593.8707581	3532.37±1.36	0.174	32.43	6749.38
2456594.7546831	3531.44±1.46	0.169	32.42	6753.41
2456594.8060264	3527.69±1.57	0.174	34.27	6748.10
2456596.6972805	3527.60±1.32	0.173	24.39	6762.69
2456596.8585212	3526.84±1.75	0.170	27.56	6747.78
2456599.7447303	3526.40±1.04	0.171	30.20	6743.89
2456599.8591416	3524.32±1.34	0.171	23.41	6745.79
2456600.8594907	3525.48±1.03	0.170	25.14	6741.79
2456601.7290393	3528.45±0.92	0.173	28.60	6746.62
2456601.8378834	3525.90±0.79	0.169	27.63	6739.36
2456602.7714141	3525.90±1.04	0.168	32.24	6742.33
2456604.8350746	3525.25±0.96	0.169	31.53	6739.14
2456608.8439887	3523.29±1.30	0.172	27.65	6743.17
2456610.6894263	3522.93±1.07	0.169	27.50	6739.51
2456610.8735256	3521.37±1.10	0.171	30.97	6737.86
2456612.7502127	3527.77±1.10	0.174	33.52	6740.98
2456612.8583272	3526.78±1.12	0.172	29.80	6738.38
2456613.6797479	3529.07±1.22	0.169	28.03	6735.98
2456613.8119367	3526.60±1.27	0.171	24.17	6743.79
2456614.6882999	3531.03±0.93	0.170	27.78	6748.94
2456614.8534636	3530.97±0.88	0.170	26.26	6742.29
2456616.7207968	3536.57±1.04	0.175	31.38	6749.62
2456616.8313997	3534.77±1.01	0.174	28.86	6745.30
2456617.6567663	3535.31±1.15	0.176	29.28	6748.42
2456617.7938856	3535.82±1.13	0.175	27.73	6750.32
2456618.6626320	3540.55±1.05	0.178	29.50	6751.19
2456618.7062435	3538.81±0.94	0.173	28.45	6754.25
2456619.7046552	3532.96±1.00	0.174	27.55	6745.56
2456619.7752114	3530.89±1.03	0.177	29.71	6753.46
2456620.6982402	3528.84±1.51	0.169	27.96	6751.00
2456620.7760071	3531.28±1.37	0.174	33.57	6756.66

In the top panels of Fig. 1 we show the posterior probability densities as functions of period for tempered Markov chain samplings employing three different $k = 1$ signal (keplerian) models. We can see that there appears to be three regions in the period space where the Markov chains identified considerable maxima for the pair of one-component moving average (MA(1)) models (middle and right columns) and only one region for the white noise model (left column). The most significant of these, i.e. the global maximum, was found to be at 25.6 days in all models. The existence of the local maxima means we are likely to find other significant periodic signals in the data.

The panels in the middle row in Fig. 1 show what we find when applying the $k = 2$ signal models, the first one being at a period of 25.6 days. This time the most significant maximum is found to be at 18.35 days when dealing with the red-noise and also including the correlation terms, in excellent agreement with the pair of signals published previously in Jenkins et al. (2013b). Therefore, we can confirm that there are two significant frequencies in the extended timeseries data for HD41248. The log-Bayesian evidences for these model comparisons can be found in Table 2 listed as Full Data Set. It can be seen that the white noise model search (left panel) did not find a unique second periodicity since it is masked by the correlated noise, variability related to activity, and increased jitter. Santos et al. (2014) could not confirm this second signal in their data and it is likely that this was due to inadequate noise modeling as they assumed a white noise model, fixed the excess white noise to an value of 0.7 ms^{-1} , and relied on analyses of model residuals that cause severe biases to the obtained solutions (Tuomi 2012; Tuomi & Anglada-Escudé 2013). We also note that the parameter density widths for both signals decrease significantly by including this new data, a feature not expected from a quasi-static source. Furthermore, the linear trend applied to the data in Santos et al. (2014) is not significant, agreeing well with zero within any reasonable confidence level (Table 2).

When employing the $k = 2$ models a second significant peak around 13 days was found to cross the 10% probability threshold in the analysis with activity correlation terms included, indicating a third signal could be present in the combined data.

Santos et al. (2014) also detected this signal and attributed it to the first harmonic of the 25 day signal, however our parameter densities suggest otherwise as the distribution did not overlap with one half of the period of the 25 day signal. In any case, we then applied the $k = 3$ models to test if this was indeed the case and we show the posterior diagrams in the bottom panels of Fig. 1. No additional signals that were unique and passed our signal detection criteria were found in the analysis. We did not employ the $k = 3$ model to the white noise model as we could not constrain any secondary signal under that assumption.

Given that no 13 day signal is found in the full data when including the noise correlations, and since the signal in the later data that we detect does not pass our planetary signal selection criteria, which are 1) the model including the signal must be 10000 times more probable than the previous model, i.e. $k + 1 \gg k$ and 2) the signal must not vary in time in period, phase, and amplitude over the baseline of the observations (see Tuomi et al. 2014b), it cannot be considered a static Doppler signal. This result is a reproduction of the same result found for the CoRoT-7 radial velocity timeseries (Tuomi et al. 2014a) where the rotation period of that star, known from the previously measured CoRoT photometry, did not correspond to a genuine velocity signal. This strongly indicates that the 13 day signal reflects a quasi-static nature that changes as a function of time and could be the actual rotational period of HD41248 or a mix of the signal from the rotational period and differential rotation. The final system parameters are listed in Table 3 and log-Bayesian evidence ratios for these tests are shown in Table 2. The phase folded signals are shown in Fig. 2.

3.1. ASAS Photometry

A large part of the problem in the signal characterisation for HD41248 surrounds the star's rotational period. Therefore, in order to see if we could pin down the rotational period we searched the latest version of the ASAS photometric catalogue (Pojmanski 1997) to see what useful data there is for HD41248 and if we could locate a plausible rotational period. We obtained V-band photometry for this star and after weeding out strong outliers (beyond $5\text{-}\sigma$) and selecting only the best

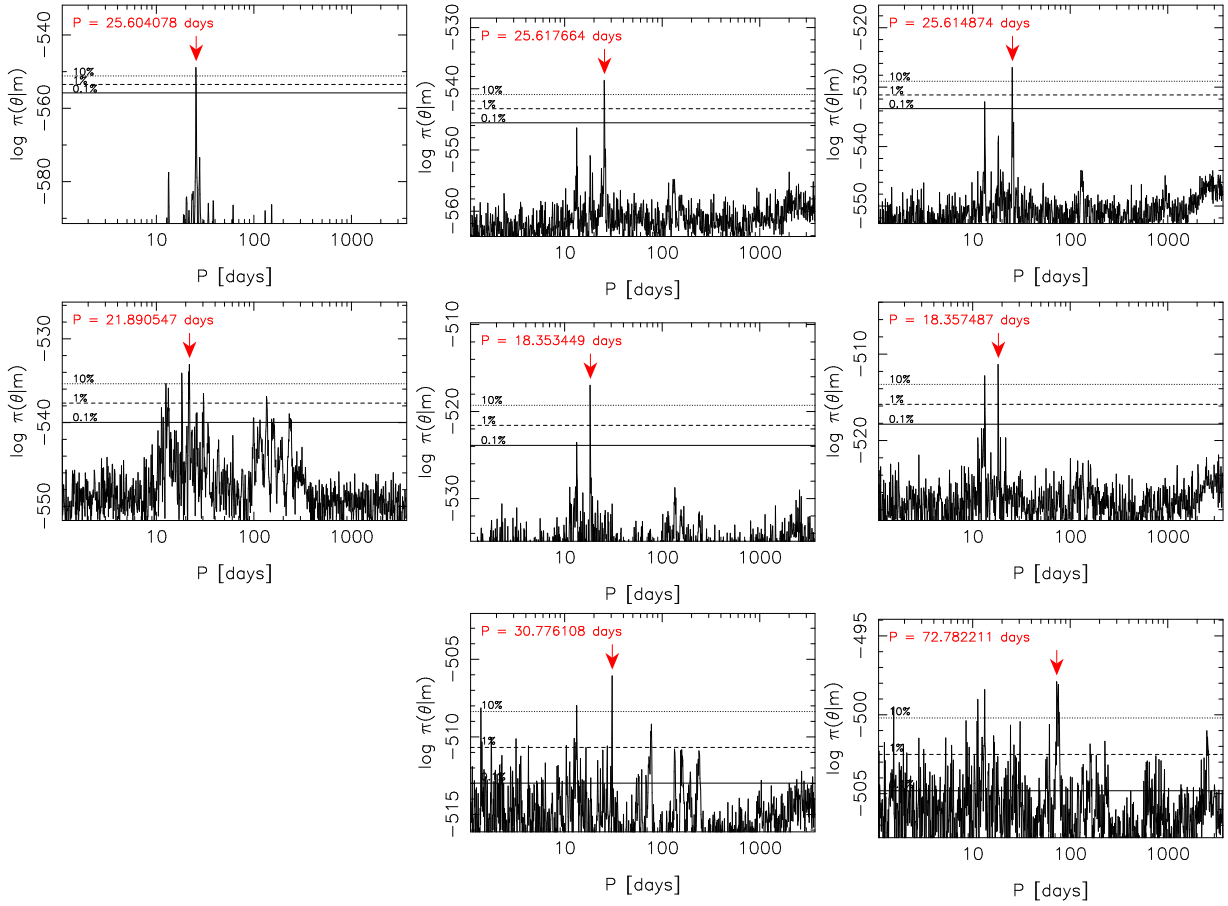


Fig. 1.— Estimated posterior probability densities based on tempered Markov chain samplings as functions of signal period. From top to bottom we show the $k=1, 2$, and 3 planet models. The maximum *a posteriori* estimates identified by the chains are highlighted on the plots, as are the 0.1, 1, and 10% equi-probability thresholds with respect to the maxima. The left column shows the pure white noise model, the middle column is for an MA(1) red-noise model without activity correlation terms included, and the right column is for an MA(1) red-noise model that includes the activity correlations. Note there is no $k=3$ planet model for the white noise model analyses (left column).

TABLE 1—*Continued*

BJD	RV [ms ⁻¹]	S-index [dex]	BIS [ms ⁻¹]	FWHM [ms ⁻¹]
2456622.6838006	3526.40±1.42	0.169	19.42	6756.13
2456623.7458227	3525.46±0.98	0.174	24.04	6742.54
2456623.8656385	3525.04±1.03	0.170	23.45	6748.55
2456624.6414198	3524.73±1.27	0.171	29.66	6741.04
2456624.7668605	3522.75±1.17	0.169	34.98	6733.78
2456626.6156583	3525.44±1.25	0.175	29.43	6741.58
2456626.8487502	3523.88±1.10	0.170	28.93	6739.69
2456627.6233271	3524.30±1.10	0.168	30.72	6742.43
2456627.8381896	3524.37±0.89	0.169	24.09	6740.67
2456628.6101737	3524.76±2.28	0.166	27.97	6745.50
2456628.8421543	3526.22±1.49	0.174	25.51	6739.56
2456629.6267424	3526.08±1.74	0.165	34.21	6744.21
2456629.8238847	3526.80±1.21	0.171	32.54	6740.69
2456630.6085999	3527.11±1.47	0.168	36.99	6746.40
2456631.6333972	3527.87±1.02	0.167	31.01	6747.34
2456631.8450650	3523.59±1.08	0.168	29.85	6739.82
2456632.6133791	3526.43±0.98	0.172	26.77	6744.59
2456632.8576512	3523.42±1.14	0.168	23.92	6744.24

data, those classed as 'A' in the ASAS photometric grading, we were left with a total of between 420-650 photometric points processed through five ASAS V-band apertures.

Periodogram analyses of each of the aperture data revealed some significant peaks. A long period peak is found beyond 1000 days, likely attributed to the magnetic cycle of the star. Another cluster of peaks emerge around 200-300 days, peaks that also appear in the radial velocities under the assumption of pure white noise (see the left column in Fig. 1). We found neither a statistically significant peak that matched the signals we see in the radial velocity data, nor a period that could plausibly relate to the stellar rotation period.

3.2. Activity Periods

In addition to analysing the photometry we also tested the activity indices by running both periodogram analyses and posterior samplings to constrain any frequencies in these indicators that would show activity cycles that could be the source of these radial velocity variations. Santos et al. (2014) show possible correlations between the 25 day radial velocity period and similar periods in

the $\log R'_{\text{HK}}$ and the CCF FWHM measurements.

First we performed a periodogram analysis on the chromospheric activity indices, after removing 3σ outliers from the sample that, when included only served to add noise. This analysis revealed a statistically significant frequency with a period of 27.62 days, close to the radial velocity period for the primary signal in the data. We then performed the same analysis on the FWHM values, using the same data set, and we found another statistically significant periodogram peak that matched the activity index peak, having a period of 27.93 days. The period of this FWHM changed to 25.31 days when we included all the FWHM data and subtracted off a linear trend from the timeseries, closely matching the radial velocity signal. The question to answer is whether these signals are related to the radial velocity variations.

In order to answer this question, we then ran MCMC samplings under our Bayesian approach to search for the signals independently and to constrain the significance of the signals and their possible extent in period space to see if they overlap with the radial velocity periods. We found the global probability maximum in the cleaned

$\log R'_{\text{HK}}$ indices to be located at 60 days with our samplings, closely followed by a 27.7 day maximum that matched the periodogram analysis. However, neither of these signals could be detected in the data according to the signal detection criteria because their periods and amplitudes could not be constrained from above and below. This means that we cannot rule out the possibility that these maxima are in fact statistical flukes caused by the combination of random noise and data sampling coupled with correlations.

We then chose to perform the same analysis on the FWHM measurements and found the strongest frequency to be at ~ 800 days, after considering the linear trend. A cluster of probability maxima was found between 20-30 days in this analysis. However, none of these maxima corresponded to a genuine signal because they did not satisfy our signal detection criteria. Our interpretation was that the reason for the 25 day peak in the periodogram analysis was simply due to making the assumption that the noise is distributed in a Gaussian fashion, which does not appear to be the case as we find a significant red-noise component in both the S -indices and the FWHM measurements. Therefore, the 25 day peak in the activity indicators is heavily model dependent. This is in stark contrast to the radial velocity signal at 25 days which is found irrespective of the assumed noise model.

3.3. Signal Coherence

As discussed in the introduction, the signal found in the radial velocity timeseries of HD166435 only had a coherence time of around 30 days. Combining this with the bisector correlations Queloz et al. (2001) ruled out the existence of this planetary candidate. In order to test the probability that the proposed planet candidates HD41248*b* and *c* are real Doppler signals and independent from any activity correlations, we split the data up into two independent sets as a function of time. The first set was the original data published in Jenkins et al. (2013b) but analysed using our current statistical model (dataset 1) and the second (dataset 2) is the new data that is around 2.5 times larger than the first data and was added in the analysis from Santos et al. (2014). The full time baseline of data covers more than 10 years, where data set 1 spans over eight years and data set 2 covers two years, but at much higher cadence.

We analysed both sets independently and in combination and recovered two signals each time with high statistical significance. The phase, period, and amplitude of the detected signals were in agreement with that published in Jenkins et al. (2013b). Table 2 shows the results for the sample for these analyses and includes results for the full data set with and without correlations with the activity indices.

The fact we see no change in the properties of the 25 day signal between the full data and the two subsets is remarkable because the star itself does change with time. We found that the intrinsic noise, parameterised with the standard deviation of the excess white noise σ_J , increased between the old and new datasets by roughly a factor of two. For the old data, the jitter was found to be 1.3 ms^{-1} but for the new data the jitter increased to 2.6 ms^{-1} . Furthermore the data is more correlated in the second dataset, with the correlation parameter ($\phi_{1,1}$) changing from being consistent with zero for old data to being significantly clustered around a value of 0.6 in the new data, meaning the noise becomes redder in the new data also. This increase in stellar noise and correlation parameter means that the second signal at 18 days is no longer detected in the second set of data and it is likely the reason Santos et al. (2014) struggled to locate the 18 day signal as they did not account for these differences in the noise. This is also likely the reason they could not find a circular solution for the 25 day signal either. We found a circular solution by both including the eccentricity prior or assuming a flat prior, however Zakamska et al. (2011) show that there is a bias towards higher eccentricities in radial velocity surveys, a bias that our eccentricity prior helps alleviate. We also note that correlations between the activity indicators and the velocities became significant in the new data whereas these correlations were not significant in the old data set (see Jenkins et al. 2013b).

Although the 18 day signal cannot be independently detected in the new data, likely due to the fact that the star has become more active and therefore disabling the detection of this weak signal behind the increased jitter and red-noise, it is still well-supported by the new data because its significance increases considerably when comparing between the old data and the full data (see Table 2). The significance of the $k = 2$ model in-

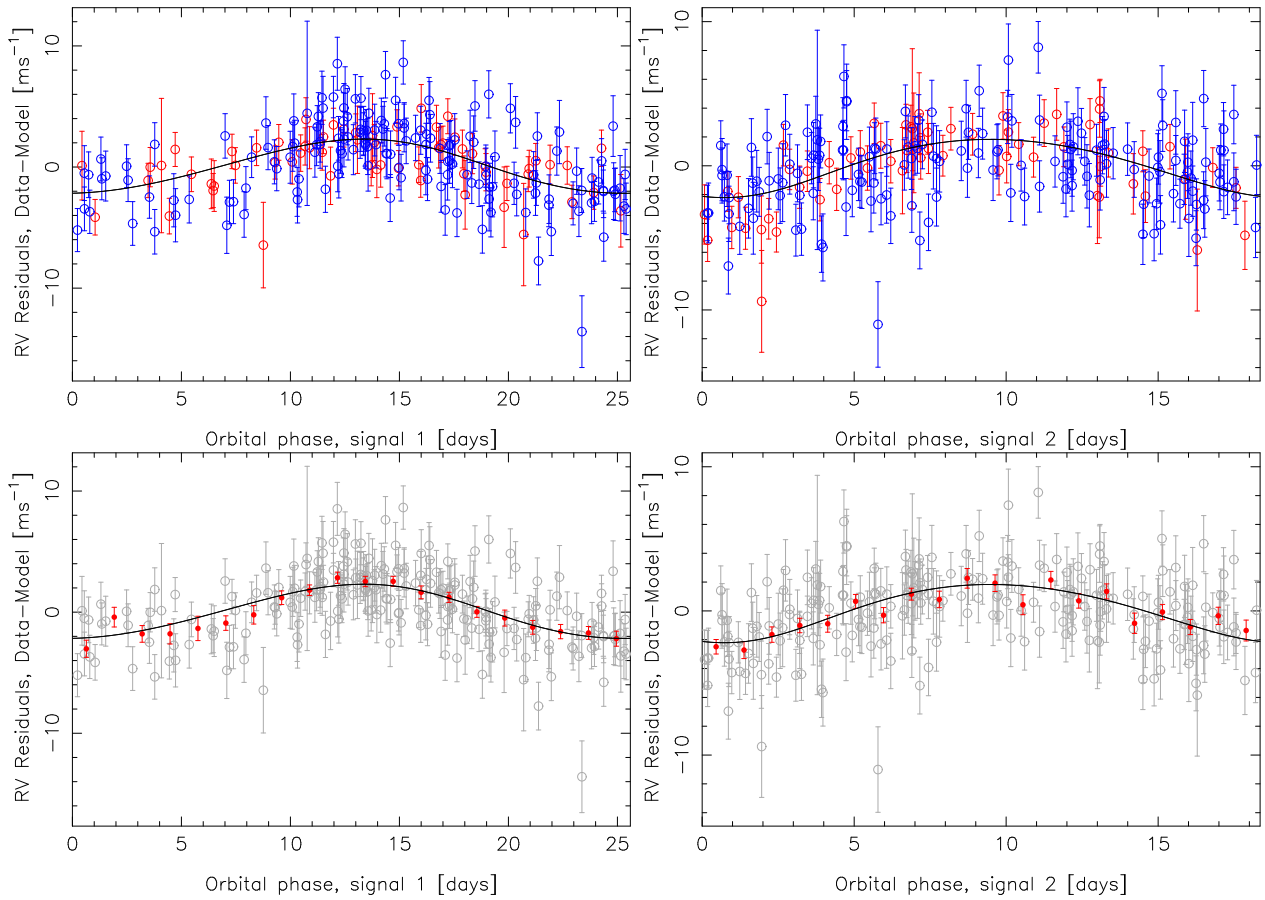


Fig. 2.— Phase folded radial velocities for both signals detected in the HD41248 radial velocities as a function of time. The red points are for old low cadence data and the blue points are for new high cadence data in the top panels. The lower panels show the same data but with filled red points representing binned velocities to highlight the significance of the signals.

creases by a factor of 2700 between the old data and the full data, where it is 1.8×10^7 times more probable than the $k = 1$ model in the full data. This means that this signal, together with the 25 day one, retain their properties throughout the data baseline and cannot be shown to be dependent on the changes in the stellar activity. This result also shows that serendipitously observing the first epoch of data when the star was intrinsically more inactive and the noise was whiter allowed both signals to be confirmed in that data set. There is the sampling cadence to consider here also, since in the first epoch of data the sampling density was lower than the later two observing seasons and it could also be that this decreased cadence helped to suppress the effects of the correlated noise.

We then split the data further into three groups so that we could examine the data sets presented in Santos et al. (2014) directly. We first consider the data published in Jenkins et al. (2013b) as one set as before (First Data), but then analyse the following two observing seasons individually, where the middle set in time runs from JD 55904.8-56414.5 and the later set runs from JD 56521.9-56632.7. Santos et al. claim that the 25 day signal amplitude evolves with time across these three observing epochs, a strong argument in favour of an activity induced signal, however we could not confirm this to be the case. What we find is a complex evolution of the properties of the data due to changes in the star and sampling. First off, we did not find any significant evidence for a change in the amplitude of the 25 day signal in the first and middle parts of the data, the amplitudes are in strong statistical agreement. We could not confirm this result on the later data since we could not constrain any signal at all in this set and below we explain why.

As discussed previously, it appears that HD41248 became more intrinsically active throughout the timeseries of this data, in agreement with findings in Santos et al. (2014), however not in a linear fashion. The jitter noise increased in the middle part of the data significantly, going from 1.3 ms^{-1} in the first part of the data, up to 2.4 ms^{-1} in the middle part, and then dropped again to 2.1 ms^{-1} for the later data, although this drop is currently not statistically significant. Added to this, the red-noise components change

with time also, going from being consistent with zero in the first and middle parts of the data to a value of 0.6 in the later data, showing an increased red-noise in the later data as well.

The activity correlations were also found to evolve throughout these three epochs of data. Again these correlations were consistent with zero in the first part of the data, for all three indicators S -index, FWHM, and BIS, but apart from the S -index whose correlations with the velocities do not appear to evolve with time, the other two indicators do. The correlations with FWHM (c_{FWHM}) go from 0.13 in the middle data to 0.16 in the later data, both values statistically consistent but also statistically different from zero. The correlations with the BIS go from being negatively correlated in the middle data, with a value of $c_{\text{BIS}} = -0.22$, and then become in agreement with zero again in the later data. Clearly the red-noise presents a complex pattern in this timeseries and when including all data after JD 55904.8, they are important and must be considered when searching for any low amplitude signals in this data. In any case, it appears that our model does a reasonable job of describing the noise in the radial velocity timeseries for HD41248, similar to the case of CoRoT-7 (Tuomi 2014).

Santos et al. (2014) claim a stable period and phase could be maintained in HD41248 by an active longitude impacting the radial velocities (Berdyugina & Usoskin 2003; Ivanov 2007), under their hypothesis that the amplitude of the signal varies with time, which we have shown here cannot be concluded to be the case. Yet Ivanov also show that although such an active longitude spot formation zones maintain their form much longer than the lifetimes of the individual spots, the solar data suggest they are only stable for 15-20 rotational periods. We show that the 25 day radial velocity signal found for HD41248 has been static for *at least* 5 years (70 rotational periods assuming the 25 day signal is the rotation period), and likely for the entire 10 year baseline of data (140 rotational periods).

As a further test we decided to again split the data up into independent sets, this time based on their chromospheric activity levels, to see if we were sensitive to the impact of the increased magnetic activity and spot formation of HD41248. We built three almost equally numbered sets, compris-

ing an inactive set ($\log R'_{\text{HK}} \leq -4.93$), an intermediately active set ($-4.93 < \log R'_{\text{HK}} \leq -4.91$), and an active set ($\log R'_{\text{HK}} > -4.91$). We proceeded to search for the 25 day signal in these data sets and found that we could detect this signal in the inactive and intermediately active sets, but could not constrain anything in the active set. This affirms why the 18 day signal cannot be detected in the later data and also calls for a noise model to be scaled as a function of chromospheric activity, an upgrade we plan to include in future versions of our model. This feature also highlights that we are sensitive to activity related features in our data and therefore, if the 25 day signal was genuinely due to rotationally modulated magnetic activity, we would expect the signal to appear stronger in the active data set than in the inactive data set, since the sensitivity to the features causing the signal increase. We might also expect it to be more significant, depending on the structure in the increased jitter noise which would also be modulated by the rotation. In any case, the signal parameters are invariant between the inactive and moderately active sets, showing that changes in the magnetic activity of the star do not change the period, amplitude, or phase of the signals, arguing against a magnetic origin for these signals.

Finally, we also tested the signals as a function of wavelength using the reddest HARPS orders only, (see Anglada-Escudé & Butler (2012) and Tuomi et al. (2013) for details), and found no dependence of the signal properties or significances on wavelength. This indicates that neither of the signals show evidence for a dependence on wavelength, at least across the wavelength domain offered by HARPS. This would again argue against the origin of these signals being from magnetic activity cycles modulated by rotation.

4. Summary

We have shown that the radial velocity time-series for the star HD41248, covering nearly 10 years of observation, clearly supports the existence of two signals with close to circular morphologies once red-noise components are considered. This analysis provides additional evidence that the pair of signals detected in this data could be due to a pair of planets in, or very near to, the 7:5 MMR with periods of 18.361 and 25.595 days

and a period ratio (P_c/P_b) of 1.394 ± 0.005 at 99% confidence level, in excellent agreement with the results published in Jenkins et al. (2013b). Such resonances are known to be a by-product of the planet formation and evolution process (Baruteau & Papaloizou 2013) in the early history of a star's life. It seems difficult to give rise to signals so close to such a period ratio simply by rotationally modulated activity in the presence of differential rotation, except in the most unique circumstances.

By analysing the signals as a function of time in an independent fashion we were able to obtain evidence for their static nature over the full baseline of observations. This analysis also allowed us to show that the star got intrinsically more active within the period of the most recent data, with the jitter noise taking on a value twice that reported in Jenkins et al. (2013b). The noise also got significantly redder and the linear correlations with the velocities and FWHM increased such that they became statistically significant over the last two observing seasons. Splitting the data further revealed a complex pattern of evolving red-noise and activity correlations, both of which would serve to mask weak signals under a white noise assumption. We conclude that noise correlations must be taken into account when attempting to search for periodic signals that are at the noise level of the star/instrument combination.

We analysed the radial velocities with and without activity indicator correlations and found that both signals are supported by the old and new HARPS velocity data. Moreover, the significances of the signals increase when including the new data and when considering the activity indicator correlations. This is characteristic behaviour of a pair of static Doppler signals. Including the linear correlation terms and red-noise correlations also results in removing spurious peaks from the white noise model search, peaks that appear in the activity indicators. We also show that the signals in the activity indicators are highly model dependent, only peaking at 25 days when gaussian noise is assumed, whereas the 25 day signal in the radial velocity measurements is found no matter what the assumption of the noise is.

Further tests revealed that we are sensitive to changes in the magnetic activity and we found that we could detect the 25 day signal in the radial

Table 3: Solutions for HD41248.

Parameter	HD41248 <i>b</i>	HD41248 <i>c</i>
P (d)	25.595 [25.551, 25.652]	18.361 [18.337, 18.392]
K (ms^{-1})	2.30 [1.39, 3.21]	1.95 [0.99, 2.83]
e	0.09 [0, 0.26]	0.10 [0, 0.28]
ω (rad)	0.3 [0, 2π]	3.3 [0, 2π]
M_0 (rad)	3.7 [0, 2π]	5.6 [0, 2π]
a (AU)	0.166 [0.148, 0.180]	0.132 [0.118, 0.146]
$m_p \sin i$ (M_\oplus)	9.8 [5.9, 14.6]	7.6 [3.6, 11.6]
	Old data	New data
τ (d)	16.8 [0, 100]	1.4 [0, 100]
ϕ	0.17 [-0.47, 0.87]	0.35 [0.10, 0.73]
σ_J (ms^{-1})	1.10 [0.77, 2.12]	2.25 [1.74, 2.81]
c_{BIS}	-0.05 [-0.29, 0.19]	-0.11 [-0.28, 0.07]
c_{FWHM}	0.03 [-0.09, 0.14]	0.13 [0.02, 0.26]
c_{S} ($\text{ms}^{-1}\text{dex}^{-1}$)	91 [-135, 343]	67 [-93, 226]
$\dot{\gamma}$ ($\text{ms}^{-1}\text{year}^{-1}$)	0.04 [-0.30, 0.37]	

velocities of the star when it was in its most inactive and moderately active states. No signals were detected when the star was in its most active state, contrary to what would be expected if these signals were due to magnetic activity since we might expect these signals to be strongest when the star is in an active state as the source of the signals should give rise to a stronger signal. We also note that the signals are independent of wavelength in the band covered by HARPS, a further argument against the magnetic activity cycle argument.

Additional confirmation that these signals could represent a pair of resonant planets may have to wait until future instruments operating in the near infrared come online. Instruments like HPF (Ramsey et al. 2008; Mahadevan et al. 2012) or CARMENES (Quirrenbach et al. 2012) could search for a change in the period or amplitudes of these signals as a function of wavelength over a much wider waveband than that offered by HARPS, which would attribute them to rotationally modulated spots on the surface of the star. Future direct imaging systems like the previously proposed TPF or Darwin missions (see Léger 2000), could be another way to confirm or not the existence of these planets, yet this type of mission is a long way off in the future and the distance of 52 pc to HD41248 makes this a real challenge. In any case, more high cadence velocity observations over the coming years might be

able to shed some light on the nature of these signals, either by searching for variations in the periods, amplitudes, and phases, or by confirming the nature of these signals with more high quality data. HD41248 therefore represents a very interesting target to monitor radial velocity signals buried within evolving red-noise and activity correlations.

JSJ and MT acknowledge funding from CATA (PB06, Conicyt). We also acknowledge the helpful and quick response from the anonymous referee.

REFERENCES

- Anglada-Escudé, G. & Butler, R. P. 2012, *ApJS*, 200, 15
- Anglada-Escudé, G., Tuomi, M., Gerlach, E., et al. 2013, *A&A*, 556, A126
- Baluev, R. V. 2013, *MNRAS*, 429, 2052
- Baruteau, C. & Papaloizou, J. C. B. 2013, *ApJ*, 778, 7
- Berdyugina, S. V. & Usoskin, I. G. 2003, *A&A*, 405, 1121
- Boisse, I., Bouchy, F., Hébrard, G., et al. 2011, *A&A*, 528, A4
- Dumusque, X., Pepe, F., Lovis, C., et al. 2012, *Nature*, 491, 207

- Hatzes, A. P. 2013a, *Astronomische Nachrichten*, 334, 616
- Hatzes, A. P. 2013b, *ApJ*, 770, 133
- Ivanov, E. V. 2007, *Advances in Space Research*, 40, 959
- Jenkins, J. S., Jones, H. R. A., Pavlenko, Y., et al. 2008, *A&A*, 485, 571
- Jenkins, J. S., Jones, H. R. A., Tinney, C. G., et al. 2006, *MNRAS*, 372, 163
- Jenkins, J. S., Jones, H. R. A., Tuomi, M., et al. 2013a, *ApJ*, 766, 67
- Jenkins, J. S., Murgas, F., Rojo, P., et al. 2011, *A&A*, 531, A8
- Jenkins, J. S., Tuomi, M., Brasser, R., Ivanyuk, O., & Murgas, F. 2013b, *ApJ*, 771, 41
- Léger, A. 2000, *Advances in Space Research*, 25, 2209
- Mahadevan, S., Ramsey, L., Bender, C., et al. 2012, in *Society of Photo-Optical Instrumentation Engineers (SPIE) Conference Series*, Vol. 8446, *Society of Photo-Optical Instrumentation Engineers (SPIE) Conference Series*
- Mayor, M., Bonfils, X., Forveille, T., et al. 2009, *A&A*, 507, 487
- Mayor, M., Pepe, F., Queloz, D., et al. 2003, *The Messenger*, 114, 20
- Pepe, F., Lovis, C., Ségransan, D., et al. 2011, *A&A*, 534, A58
- Pojmanski, G. 1997, *Acta Astron.*, 47, 467
- Queloz, D., Henry, G. W., Sivan, J. P., et al. 2001, *A&A*, 379, 279
- Quirrenbach, A., Amado, P. J., Seifert, W., et al. 2012, in *Society of Photo-Optical Instrumentation Engineers (SPIE) Conference Series*, Vol. 8446, *Society of Photo-Optical Instrumentation Engineers (SPIE) Conference Series*
- Ramsey, L. W., Barnes, J. R., Redman, S. L., et al. 2008, *PASP*
- Santos, N. C., Mortier, A., Faria, J. P., et al. 2014, *ArXiv e-prints*
- Tuomi, M. 2012, *A&A*, 543, A52
- Tuomi, M. 2014, *MNRAS*
- Tuomi, M. & Anglada-Escudé, G. 2013, *A&A*, 556, A111
- Tuomi, M., Anglada-Escudé, G., Gerlach, E., et al. 2013, *A&A*, 549, A48
- Tuomi, M., Anglada-Escudé, G., Jenkins, J. S., & Jones, H. R. A. 2014a, *ArXiv e-prints*
- Tuomi, M., Jones, H. R. A., Barnes, J. R., Anglada-Escudé, G., & Jenkins, J. S. 2014b, *MNRAS*, 441, 1545
- Udry, S., Bonfils, X., Delfosse, X., et al. 2007, *A&A*, 469, L43
- Vogt, S. S., Butler, R. P., & Haghighipour, N. 2012, *Astronomische Nachrichten*, 333, 561
- Vogt, S. S., Butler, R. P., Rivera, E. J., et al. 2010, *ApJ*, 723, 954
- Zakamska, N. L., Pan, M., & Ford, E. B. 2011, *MNRAS*, 410, 1895

Table 2: Log-Bayes factors $\ln B_{1,0}$ and $\ln B_{2,1}$, i.e. in favour of one against zero and in favour of two against one-Keplerian models, given various divisions of the data and different models. The last column denotes the periods of the significantly detected signals. The models contain a moving average component. Two alternative two-Keplerian solutions are shown for the full data set.

Data/Model	1	2	Periods [d]
Old Data	18.4	8.8	25, 18
New Data	13.8	–	25
Full Data	21.8	15.2	25, 18
Full Data with Activity Correlations	22.8	16.7	25, 18